

## A 3-D IMAGE REGISTRATION METHOD FOR DYNAMIC SUBTRACTION OF MAGNETIC RESONANCE LIVER VOLUMES

L.T. Mainardi\*<sup>^</sup>, K.M. Passera\*<sup>^</sup>, A. Lucesoli\*\*<sup>^</sup>, P. Potepan\*\*\*<sup>^</sup>, E.Setti\*\*<sup>^</sup>, D. Vergnaghi\*\*\*<sup>^</sup>.

\* Department of Biomedical Engineering, Polytechnic University of Milan, Italy

\*\* Department of Electromagnetism and Bioengineering, Marche Polytechnic University, Italy

\*\*\* Department of Imaging Diagnosis and Radiotherapy, National Cancer Institute of Milan, Italy

<sup>^</sup> Laboratory of Advanced Radiological Image Analysis (LARA), Milano, Italy

luca.mainardi@biomed.polimi.it

**Abstract:** In this work we present a novel realignment method for 3D Magnetic Resonance (MR) contrast-enhanced liver images acquired before and after contrast agent injection. Our method combines a rigid registration, based on Normalized Mutual Information (NMI) maximization and an elastic registration, based on a multiresolution analysis performed through Wavelet Transform. The method is validated using numerical indexes and clinical score. A few examples will be shown to document the clinical implementation of the method.

### Introduction

Gadolinium-enhanced MR imaging is a very important diagnostic tool for the detection and characterization of primary and secondary focal liver lesions [1]. Intensity changes between images acquired before and after Gadolinium injection are emphasised by a subtraction technique [2].

Nevertheless subtraction between liver volumes is not trivial, because volumes can shift during different exam phases as effect of patients movements or merely as a consequence of respiratory activity.

In this article, a 3D MR contrast-enhanced liver images registration method is described. Medical images registration problem was faced by different authors [3], however the complexity of MR dynamic images of liver makes the use of many of these methods not adequate. Difficulties are related to the fact that liver is subjected to large shifts during respiration and to the impossibility to define reliable external and internal landmarks for evaluating liver displacements [3].

Recently a novel elastic method has been proposed, for breast contrast-enhanced images registration [5]. It is based on Complex Discrete Wavelet Transform (CDWT) decomposition using Gabor-like filters. It was initially proposed as an efficient tool to obtain a multiresolution motion field estimation ( $\mathbf{f}$ ) between two subsequent video frames [6]-[8]. At each scale,  $\mathbf{f}$  is obtained as the minimum of a quadratic surface, named Subband Square Difference (SSD) [6], defined by CDWT coefficients. Minimising SSD is approximately equivalent to maximising the phase correlation among pixels. In addition, it can be proved that SSD is a

Maximum Likelihood (ML) estimator of the motion field  $\mathbf{f}$  [8]. Finally, the method is completely automatic and it doesn't require the use of external or internal landmarks.

The application of this algorithm for breast images has been demonstrated to be suitable to register medical soft tissues images, overcoming limitations imposed by rigid registration [3]. The method is computationally efficient and nearly insensitive to intensity variations due to contrast injection [5].

Realignment of MR liver volumes is more complex. In fact liver is the most floating abdominal organ [9], with an estimated excursion of about 5.5 cm in deep respiration, 2.5 cm in normal respiration and 0.9 cm during breath-holding.

To minimise this problem the dynamic MR acquisition is realised during breath suspension. Nevertheless volumes obtained in different phases show misregistration caused by the unequal patients breath-hold during acquisitions.

This misregistration has a macroscopic rigid component in cranio-caudal direction and a smaller one, due to the fact that liver, as a soft tissue, may deform in a non-rigid way.

In order to compensate these effects, we designed a method composed by a two-steps registration: a first rigid registration in cranio-caudal direction is followed by an elastic registration within slices. The rigid registration, based on Normalized Mutual Information (NMI) [10] maximization, guarantees an anatomical section correspondence among slices of the two image volumes. The subsequent elastic registration, based on CDWT, has the goal to locally refine the rigid realignment.

In this work the registration method, its validation and some examples of liver MR volumes alignment are presented and discussed.

### Materials and Methods

*Experimental protocol.* The algorithm has been tested as a part of an experimental protocol developed at the Department of Images of the National Cancer Institute of Milan, in the period from September to November 2004. Twelve clinical cases were examined. Patients age ranged from 37 to 67 (median 45). All

patients have been evaluated by volumetric T1-weighted gradient echo fat saturated acquisition in addition to 2D routine sequences. Volumetric T1-weighted sequences (VIBE, TR 5.2 ms, TE 2.6 ms, flip angle 20°, slice thickness 1.5 mm) have been acquired by a 1.5 T scanner before and 45 s after contrast agent injection. The acquisition parameters were optimised in order to find a better enhancement of the portal system. Slices number varies from 70 to 112 slices per volume with relation to liver size. Patients received 0.2 mmol/kg of paramagnetic contrast agent in a single bolus in a flux of 1.5-2 ml/s followed to 20 ml of physiologic solution (NaCl at the 0.09%) to favourite the contrast agent progression in the venous circle.

*Registration procedure.* The proposed method is sketched in Figure 1. It is composed of 3 stages: i) pre-processing, ii) rigid registration and iii) elastic registration. While the registration algorithms are automatic, the segmentation requires an user intervention: the method is therefore semi-automatic.

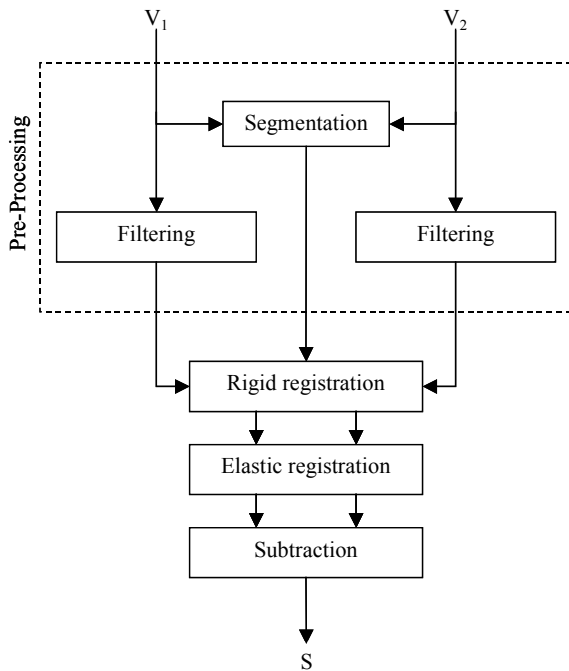


Figure 1: block diagram of the method. V1 and V2 are respectively the pre-contrast and the post-contrast volume.

i) Pre-processing: signal-to-noise ratio (SNR) in MR images is lower in case of 3D acquisition than in usual 2D acquisition [11]. An excessive noise level could make the algorithm not convergent [3] or the estimate unreliable [7]. Hence it is necessary to increase the SNR before performing the registration. Traditional filtering techniques are often unsuitable because they may introduce blurring in the images [12]. In order to obtain a compromise between noise decrease and details preservation we apply an adaptive filter whose parameters are updated on the basis of local mean and variance of image [12].

In addition, the other abdominal organs may show a relative displacement with respect to the liver [9] reducing the performance of the realignment method. These other organs are removed from the images by means of a manual segmentation of the liver [3].

ii) Rigid registration corrects the liver displacement in cranio-caudal direction, orthogonal to transverse section (z axis). In this way, corresponding slices in the two volumes represent the same anatomical liver section. The registration is performed by maximising the Normalized Mutual Information (NMI) [13] as a function of the translation along z direction:

$$NMI = \frac{H(I_1) + H(T(I_2))}{H(I_1, T(I_2))} \quad (1)$$

where  $I_1$  and  $I_2$  are respectively the pre-contrast and the post-contrast image,  $T(\cdot)$  is the translation,  $H(I_1)$  and  $H(T(I_2))$  are the entropy of  $I_1$  and  $T(I_2)$ , and  $H(I_1, T(I_2))$  is their joint entropy. NMI is largely used as similarity index between images [3] [10] [13].

iii) Elastic registration aims to compensate deformations within corresponding slices of the two volumes. Only a brief description of the method is presented here. A more detailed survey can be found in [6]-[8]. The algorithm is divided in three steps: i) CDWT decomposition, ii) motion estimation at each decomposition level, iii) *coarse-to-fine* motion field refinement.

Firstly, the images  $I_1$  and  $I_2$  are decomposed by a CDWT analysis. The decomposition, at each scale  $m$ , corresponds to the application of the following linear filters:

$$D^{(q,m)}(\mathbf{n}) = \sum_k I(\mathbf{k}) \psi^{(q,m)}(2^m \mathbf{n} - \mathbf{k}) \quad (2)$$

$$I^{(p,m)}(\mathbf{n}) = \sum_k I(\mathbf{k}) \phi^{(p,m)}(2^m \mathbf{n} - \mathbf{k}) \quad (3)$$

where  $D^{(q,m)}$   $q=\{1,2,\dots,6\}$  are the details at level  $m$ ,  $I^{(p,m)}$   $p=\{1,2\}$  are the downsampled versions of the original image  $I(\mathbf{n})$  and  $\mathbf{n}=\{n_x, n_y\}$  are the spatial coordinates.  $\psi(\mathbf{n})$  and  $\phi(\mathbf{n})$  are respectively the Gabor-like wavelet filters and the scale filters characterising the wavelet analysis. In his original work [7], Magarey selects the wavelet filters so that each subimage  $D^{(q,m)}$  has a particular orientation defined by the spatial frequency  $\Omega_{q,m}$ . In the spatial frequency domain, the ensemble of six filters cover both the first and the second quadrant, which including all the non-redundant useful information in image analysis.

After decomposition, at each level  $m$ , the motion field  $\mathbf{f}$  is computed by minimising:

$$SSD^m(\mathbf{n}, \mathbf{f}) = \sum_{q=1}^6 \frac{|D_{i,1}^{(q,m)}(\mathbf{n} + \mathbf{f}) - D_{i,2}^{(q,m)}(\mathbf{n})|^2}{P^{(q,m)}} \quad (4)$$

where  $D_{i,1}^{(q,m)}(\mathbf{n}+\mathbf{f})$  and  $D_{i,2}^{(q,m)}(\mathbf{n})$  are the subimages obtained respectively from the decomposition of  $I_1$  and  $I_2$ , and  $P^{(q,m)}$  is the wavelet filter energy. Equation (4) is known as *Subband Squared Difference* (SSD). SSD is independent from any shifting or scaling between  $I_1$  and  $I_2$  intensity. In addition (4) is demonstrated to be a maximum likelihood estimator of the motion field  $\mathbf{f}$  [7].

Thanks to the interpolability property of Gabor-like filters, SSD(m) can be rewritten as a 2D quadratic surface with elliptical contours:

$$SSD^{(m)}(\mathbf{n},\mathbf{f}) \approx \frac{1}{2}(\mathbf{f}-\mathbf{f}_0)^T \boldsymbol{\kappa}(\mathbf{f}-\mathbf{f}_0) + \delta \quad (5)$$

where  $\mathbf{f}_0$  is the local minimum,  $\boldsymbol{\kappa}$  is the curvature matrix and  $\delta$  is the surface minimum height. Surface parameters  $\{\mathbf{f}_0, \boldsymbol{\kappa}, \delta\}$  can be computed directly from  $D_{i,1}^{(q,m)}(\mathbf{n}+\mathbf{f})$  and  $D_{i,2}^{(q,m)}(\mathbf{n})$ , and the spatial frequency  $\Omega_{q,m}$  [7]. For our purposes, the most important parameter is  $\mathbf{f}_0$ , the motion field to be estimated. It is important to observe that  $\mathbf{f}_0$  is computed for each pixel  $\mathbf{n}$ , so that the motion field is elastic.

The estimate at level  $m^{max}$  is a low resolution approximation of the motion field. The estimation is refined including the information of the CDWT coefficients at the lower levels  $m < m^{max} - 1$  with a procedure called coarse-to-fine strategy. To obtain this refinement, the motion estimation and the others SSD parameters are propagated from each level  $m$  to the next level  $m-1$ . They are firstly scaled and interpolated according to the following relationships:

$$\mathbf{f}_0 \mapsto 2\mathbf{f}_0 \quad \boldsymbol{\kappa} \mapsto \boldsymbol{\kappa}/4 \quad \delta \mapsto \delta \quad (6)$$

and SSD is converted in a new SSD' consistent with the new scale. Then the parameters at level  $m-1$  are computed from the *Cumulative Squared Difference* (CSD), defined as follows:

$$CSD^{(m)} = \begin{cases} \xi CSD^{(m+1)} + SSD^{(m)} & m_{min} \leq m < m_{max} \\ SSD^{(m)} & m = m_{max} \end{cases} \quad (7)$$

namely the  $CSD^{(m+1)}$ , scaled of a weighting factor  $\xi$ , are added to  $SSD^{(m)}$  surfaces at each level  $m < m^{max}$ . The cumulative combination of surfaces makes it possible to incorporate information from all every level of detail in the estimated motion field. The procedure terminates when the minimum detail level  $m^{min}$  is reached.

## Results

The proposed method was evaluated in numerical terms through NMI computation between pre- and post-contrast volumes. We analysed improvements introduced by both rigid and elastic registration Results are summarized in Table 1. The application of the rigid registration increased NMI of about 10%. A further

improvement of about 22% was obtained by elastic registration. Increments were statistically significant.

Table 1: Quantitative performance (\*p<0.5,\*\*p<0.01)

NMI		
Original Images	After Rigid Registration	After Elastic Registration
0.069±0.024	0.076±0.026*	0.093±0.031**

It worth noting that improvements were distributed among all slices of a volume. Figure 2 shows NMI behaviour with respect to slice number. In this graph the improvement in NMI in each phase is evident. In particular, the additional increase obtained after CDWT registration proves that an elastic registration is fundamental to allow for liver deformations.

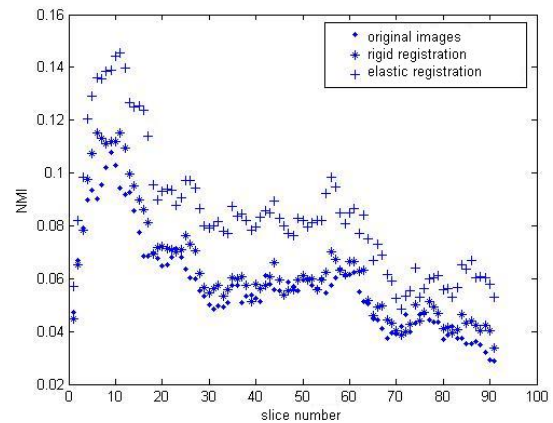


Figure 2: NMI graph.

This improvement can be appreciated in Figure 3 where a comparison of subtraction technique applied to original images (a), after rigid registration (b) and after elastic registration (c) is presented. Before registration, the subtraction image is affected by important rim artifacts at liver borders. After rigid registration artifacts diminish and it is only after the elastic registration that they vanished.

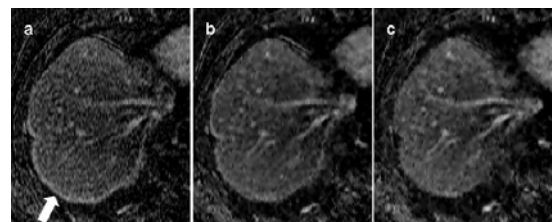


Figure 3: Comparison of subtraction images:(a) subtraction of original images, (b)subtraction after rigid registration, (c)subtraction after elastic registration. The arrow shows the rim artifact at the liver border.

In order to verify method performances in terms of clinical usability, two expert radiologists evaluated subtractions with respect to volumetric post-contrast T1-

images (VIBE). The considered image properties concern vessel detectability and lesion characterization. The clinical scores ranged from 0 to 5, five indicating the top quality. Results are summarized in Table 2, where clinical usefulness of realigned images is documented.

Table 2: Clinical features (\* $p < 0.1$ , \*\* $p < 0.01$ )

Clinical feature	VIBE	subtraction
Vessel detectability	2.83±1.10	3.05±1.05*
Lesion characterization	2.40±0.54	3.20±0.83**

Figure 4 shows liver metastatic lesions from breast cancer: in the subtraction image lesions are more easily detectable.

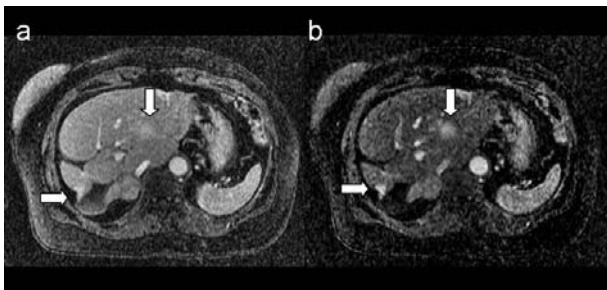


Figure 4: (a) T1-weighted 3D post-contrast image, (b) Subtraction image. The arrows show the considered lesions.

## Discussion

In literature only a few works address the problem of liver volumes registration [3]. The reason is that the problem is more complex than for other organs: liver is a soft tissue and it may deform and a simply rigid registration is often not adequate. Another difficulty concerns the presence of other organs in abdominal images that have a relative shift with respect to liver.

Nevertheless a correct registration would permit the use of a subtraction technique that is considered of potential interest in clinical practice diagnosis [2].

The method presented in this work tries to overcome these problems by combining a manual segmentation with a registration procedure composed by a rigid registration in cranio-caudal direction and a slice-to-slice elastic registration. The latest is implemented by a multiresolution analysis carried out through the CDWT Transform [6]. The numerical results show that the method is consistent and the NMI increases after realignment, in particular the elastic registration phase gives the better results.

The clinical score shows that the subtraction images obtained after registration allow a better characterization of lesions and vessels.

## Conclusions

We introduced a novel method for 3D realignment of liver MRI volumes. The method was documented to provide an efficient realignment of the liver structures allowing the use of subtraction technique between pre- and post-contrast volumes with positive benefit for the clinical image readability.

## References

- [1] KAMEL I.R., BLUEMKE D.A. (2003): 'MR imaging for liver tumors', *Radiologic Clinics of North America*, **41**, pp. 51-65.
- [2] YU J., ROFSKY N.M. (2003): 'Dynamic subtraction MR imaging of the liver: advantages and pitfalls', *American J. of Roentgenology*, **180**, pp. 1351-1357.
- [3] CARRILLO A., DUERK J.L., LEWIN J.S., and WILSON D.L. (2000): 'Semiautomatic 3-D image registration as applied to interventional MRI liver cancer treatment', *IEEE Trans. on Med. Imaging*, **19**, n°3.
- [4] ROFSKY N.M., LEE V. S., LAUB G., POLLACK M. A., KRINSKY G. A., THOMASSON D., AMBROSINO M. M., WEINREB J. C. (1999): 'Abdominal MR imaging with a Volumetric Interpolated Breath-hold examination', *Radiology*, **212**, pp. 876-884.
- [5] MAINARDI L. T., VERGNAGHI D., CATTANEO R., SETTI E., MUSUMECI R., CERUTTI S. (2002): 'A motion estimation algorithm based on complex wavelets for the realignment of dynamic MR breast images', 2nd European Medical & Biological Engineering Conference, Vienna.
- [6] MAGAREY J. AND KINGSBURY N. (1998): 'Motion estimation using a complex-valued wavelet transform', *IEEE Transactions on Signal Processing*, **46(4)**, pp. 1069-1084.
- [7] MAGAREY J. (1997): 'Motion Estimation using Complex Wavelets', Ph.D. thesis, University of Cambridge.
- [8] MAGAREY J. AND KINGSBURY N. (1995): 'Motion estimation using complex wavelets', Technical Report TR-226, Cambridge University Engineering Department.
- [9] SURAMO I., PÄIVÄNSALO M., MYLLYLÄ V. (1984): 'Cranio-caudal movements of the liver, pancreas and kidneys in respiration', *Acta Radiologica Diagnosis*, **25(2)**.
- [10] VIOLA P. AND WELLS W. M. (1997): 'Alignment by Maximization of Mutual Information', *International Journal of Computer Vision*, **24(2)**, pp. 137-154.
- [11] MACOVSKI A. (1996): 'Noise in MRI', *Magn. Reson. Med.*, **36**, pp. 494-497.
- [12] LUO S., HAN J. (2001): 'Filtering medical image using adaptative filter', *Proceedings of the 23rd Annual EMBS International Conference, Istanbul, Turkey*, pp. 25-28.
- [13] PLUIM J.P.W., MAINTZ J.B.A., VIERGEVER M.A. (2003): 'Mutual Information Based Registration of Medical Images: A Survey', *IEEE Trans on Medical Imaging*.